N_{Re} = Reynolds number = $2Rv\rho/\mu$, dimensionless
p = pressure, dyne/sq.cm.
r = radius, cm.
R = radius of fall tube, cm.
v_r, v_r^0, v_z, v_z^0 = axisymmetric cylindrical velocity component, cm./sec.
v_0 = theoretical terminal velocity without end effects, cm./sec.
v_1 = theoretical terminal velocity with end effects, cm./sec.
v_2 = experimental terminal velocity, cm./sec.
z = distance, cm.

Greek Letters

β_0 = viscometer constant, theoretical, sq.cm.
β_2 = viscometer constant, experimental, sq.cm.
β_r = viscometer constant, reduced, dimensionless
κ = radius of falling cylinder/radius of fall tube, dimensionless
μ = viscosity, g./(cm.)(sec.)
ρ = density of oil, g./cu.cm.
σ = density of cylinder, g./cu.cm.
Φ_v' = axisymmetric velocity dissipation function, 1/sec.^{2}
Ψ_{ee} = theoretical end effects coefficient, dimensionless

LITERATURE CITED

1. Ashare, Edward, R. B. Bird, and J. A. Lescarboura, *AIChE J.*, 11, 910 (1965).
2. Bird, R. B., W. E. Stewart, and E. N. Lightfoot, "Transport Phenomena," Wiley, N.Y. (1964).
3. Chen, M. C. S., J. A. Lescarboura, and G. W. Swift, *AIChE J.*, 14, 123 (1968).
4. Chen, M. C. S., Ph.D. dissertation, Univ. Kansas, Lawrence (1970).
5. Eichstadt, F. J., and G. W. Swift, *AIChE J.*, 12, 1179 (1966).
6. Huang, E. T. S., G. W. Swift, and F. Kurata, *AIChE J.*, 12, 932 (1966).
7. Kantorovich, L. V., and V. I. Krylov, "Approximate Methods of Higher Analysis," Interscience, N.Y. (1958).
8. Lohrenz, J., G. W. Swift, and F. Kurata, *AIChE J.*, 6, 547 (1960).
9. Schechter, R. S., "The Variational Method in Engineering," McGraw-Hill, N.Y. (1967).
10. Swift, G. W., J. Lohrenz, and F. Kurata, *AIChE J.*, 6, 415 (1960).
11. Walker, J. D., Ph.D. dissertation, Univ. Kansas, Lawrence (1970).

Manuscript received May 28, 1970; revision received July 16, 1971; paper accepted August 2, 1971.

Non-Newtonian Behavior of a Suspension of Liquid Drops in Tube Flow

W. A. HYMAN and RICHARD SKALAK

Department of Civil Engineering and Engineering Mechanics
Columbia University, New York, New York 10027

This paper presents an analysis and computed results of the flow of deformable droplets of one Newtonian fluid suspended in another Newtonian fluid. Surface tension is assumed to act at the interface of the two fluids. Non-Newtonian characteristics of the suspension are demonstrated and are qualitatively similar to flow characteristics of blood in capillaries.

The results show that the deformation of the drops may result in a significant reduction in the pressure gradient compared with that necessary for a suspension of rigid spheres or spherical (nondeformable) liquid drops. The decrease in the pressure gradient is velocity dependent. This constitutes a mechanism of non-Newtonian behavior of the suspension as a whole, and is attributable to the flexibility of the suspended elements. The resultant shapes of the liquid drops are similar to the shapes of red blood cells that have been observed in narrow glass capillaries as well as in blood vessels.

This study considers the axisymmetric flow of a suspension of deformable liquid drops through a rigid cylindrical tube (Figure 1). The liquid in each drop and the suspending fluid are both assumed to be Newtonian and incompressible. A surface tension is assumed to act at the interface. The analysis allows for an arbitrary ratio of viscosity of the liquid drops to that of the suspending fluid. The motion is assumed to be sufficiently slow so that inertial terms in the equation of motion may be neglected.

This system is considered to be a possible model of blood flow in the capillaries. The liquid drops of the present

W. A. Hyman is at the Department of Mechanical Engineering, Massachusetts Institute of Technology, Cambridge, Massachusetts 02139.

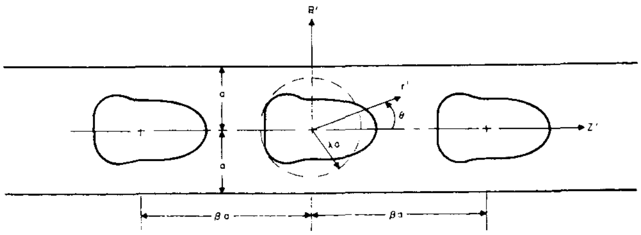

Fig. 1. Geometry of the system.

model represent the red and white blood cells and the suspending fluid represents the blood plasma. As a result of the surface tension assumed, the liquid drops will be spherical when at rest. Red blood cells (erythrocytes) are flexible biconcave disks containing a concentrated solution of hemoglobin within a thin membrane. The diameter of a red blood cell is approximately 8 μ, and its thickness is about 2.5 μ. White blood cells are more nearly spherical, and are characterized by a high internal viscosity. The blood plasma, while also a suspension, does not exhibit the same non-Newtonian behavior as blood itself. Plasma is well represented as a Newtonian fluid with viscosity approximately 1.8 cp. Small capillaries have diameters of the same order as the diameter of red cells, and are relatively rigid with respect to physiological pressures. Capillary lengths are in the range of 100 to 1,000 μ and the mean velocity of flow in capillaries is of the order of 1 min./sec. The Reynolds number of a typical capillary flow is less than 10^{-2}.

Although the present model is not an accurate representation of blood flow, it does contain sufficient parallels to be of value. Perhaps the most serious deficiency, apart from geometry, is the use of a fluid-fluid interface with surface tension to represent the fluid-membrane-fluid boundary. The model requires the matching of fluid velocities at the boundary which creates a steady circulation inside the drops. The membrane of a red blood cell would be stationary in steady axisymmetric flow, and there would be no internal motion. The steady state shape of the drops is found to depend primarily on the normal stresses at the interface. The effect of normal stresses in deforming a red cell will be qualitatively similar.

The present model is realistic for blood flow in the assumptions of a rigid tube, a Newtonian suspending fluid, inertia-free flow (Reynolds number $<< 1$), and, to a lesser degree, in the membrane behavior.

Since the specific gravity of red cells is about 1.10 and that of plasma 1.03, the buoyant force on a red cell is small in typical capillary flow. In the theory presented, the liquid drops are assumed to be neutrally buoyant.

The specific problem treated is illustrated in Figure 1. An infinite row of equally spaced fluid drops, of viscosity μ_i and density ρ_i, are assumed to be undergoing axial translation in an infinite, rigid, circular cylinder containing a second fluid of viscosity μ and density ρ. The system has a discharge Q consisting of both liquid drops and the suspending fluid. It is assumed that each drop and the flow of the suspending fluid are axisymmetric.

The geometry of the problem is determined by the tube radius a, the drop spacing βa, and the volume of the drop $\frac{4}{3}\pi(\lambda a)^3$. The total discharge and the properties of the two fluids are assumed to be known. It has been shown that the flow is then unique (*1*).

A number of studies have considered the effect of a cylindrical tube on the flow of long bubbles whose length is much greater than the tube diameter (*2* to *5*). The case of a single spherical drop in an infinite tube was considered by Haberman and Sayre (*6*). Wang and Skalak (*7*) treated the case of an infinite line of rigid spheres in a cylindrical tube. These results have been extended (*8*) to include the case of liquid drops which remain spherical due to a sufficiently high surface tension. In the present problem the drop shapes are not restricted and large deformations occur.

Unlike the previous studies, the problem is no longer linear with respect to the discharge Q. The extent of the droplet deformation depends on the discharge and the pressure drop is in turn dependent on droplet shape.

FORMULATION

For the steady, slow, viscous flow of an incompressible fluid, the equations of motion and continuity are

$$-\frac{1}{\rho}\nabla' p' + \nu\nabla'^2\mathbf{V}' = 0 \qquad (1)$$

$$\nabla' \cdot \mathbf{V}' = 0 \qquad (2)$$

The equations are nondimensionalized by using the tube radius a and the outside fluid properties ρ, ν, as follows. Let

$$\mathbf{V} = \frac{a\mathbf{V}'}{\nu}, \quad p = \frac{a^2}{\rho\nu^2}p', \quad \tau = \frac{a^2\tau'}{\rho\nu^2}$$

$$Q = \frac{Q'}{a\nu}, \quad D = \frac{D'}{\rho\nu^2}, \quad \psi = \frac{\psi'}{a\nu} \qquad (3)$$

The ratio

$$\sigma = \frac{\mu_i}{\mu} \qquad (4)$$

is also introduced where the subscript i stands for values inside a drop.

In the present case of axisymmetric flow, Equation (1) leads to a fourth-order partial differential equation on the stream function (*9*):

$$E^4\psi = 0 \qquad (5)$$

In spherical coordinates (r, θ)

$$E^4 = \left(\frac{\partial^2}{\partial r^2} + \frac{1-\eta^2}{r^2}\frac{\partial^2}{\partial \eta^2}\right)^2 \qquad (6)$$

where $\eta = \cos\theta$. The velocity components are given by

$$V_r = \frac{1}{r^2}\frac{\partial\psi}{\partial\eta}, \quad V_\theta = \frac{(1-\eta^2)^{-1/2}}{r}\frac{\partial\psi}{\partial r} \qquad (7)$$

In cylindrical coordinates (R, Z)

$$E^4 = \left(\frac{\partial^2}{\partial Z^2} + \frac{\partial^2}{\partial R^2} - \frac{1}{R}\frac{\partial}{\partial R}\right)^2 \qquad (8)$$

and

$$V_Z = -\frac{1}{R}\frac{\partial\psi}{\partial R}, \quad V_R = \frac{1}{R}\frac{\partial\psi}{\partial Z} \qquad (9)$$

The discharge Q in terms of the stream function ψ is given by

$$Q = -2\pi[\psi]_{R=1} \qquad (10)$$

where $[\Psi]_{R=0}$ is taken to be zero for convenience.

Consider now a coordinate system moving in the positive Z direction at velocity U, which is the velocity of the centroid of the liquid drops. In this coordinate system, the boundary conditions on the cylindrical wall ($R = 1$) are

$$V_Z = -U$$
$$\psi = = -\frac{Q}{2\pi} + \frac{U}{2} \tag{11}$$

The boundary conditions on the surface of each drop, for a steady state solution, are

$$\begin{aligned} V_n &= 0 \\ V_{ni} &= 0 \\ V_t &= V_{ti} \\ \tau_{nt} &= (\tau_{nt})_i \\ \tau_{nn} &= (\tau_{nn})_i + \delta H \end{aligned} \tag{12}$$

where n is the direction normal to the drop surface and t is the direction tangential to the drop surface in a meridonal plane. H is the dimensionless mean curvature, expressed by

$$H = aH' = a\left(\frac{1}{R'_1} + \frac{1}{R'_2}\right) \tag{13}$$

For an axisymmetric surface the principal radii of curvature are the radius of curvature of the generating curve in a meridional plane, and the distance from a point on the curve to the axis measured along the normal through that point (*10*). In Equation (12) δ is a dimensionless surface tension

$$\delta = \frac{a\delta'}{\rho\nu^2} \tag{14}$$

The boundary conditions can be expressed in terms of components of velocity and stress referred to spherical coordinates through the transformation equations:

$$\begin{aligned} V_t &= V_\theta \cos\alpha + V_r \sin\alpha \\ V_n &= V_r \cos\alpha - V_\theta \sin\alpha \\ \tau_{nt} &= (\tau_{rr} - \tau_{\theta\theta}) \sin\alpha \cos\alpha + \tau_{r\theta} (\cos^2\alpha - \sin^2\alpha) \\ \tau_{nn} &= \tau_{rr} \cos^2\alpha + \tau_{\theta\theta} \sin^2\alpha - 2\tau_{r\theta} \sin\alpha \cos\alpha \end{aligned} \tag{15}$$

If the surface of the drop enclosing the origin is described by specifying the radius as a function $r_0(\theta)$, then

$$\alpha = \tan^{-1}\left(\frac{1}{r_0}\frac{dr_0}{d\theta}\right) \tag{16}$$

In terms of r_0 the expression for H becomes

$$H = \left\{2 + 2\left(\frac{1}{r_0}\frac{dr_0}{d\theta}\right)^2 - \frac{d}{d\theta}\left(\frac{1}{r_0}\frac{dr_0}{d\theta}\right) - \left(\frac{1}{r}\frac{dr_0}{d\theta} + \left(\frac{1}{r_0}\frac{dr_0}{d\theta}\right)^3\right)\cot\theta\right\} \cdot \left\{r_0 + \frac{1}{r_0}\left(\frac{dr_0}{d\theta}\right)^2\right\}^{-3/2} \tag{17}$$

The surfaces at which the boundary conditions [Equations (12)] are to be applied are not known a priori but must be found as part of the solution. The technique used here to accomplish this involves obtaining a sequence of quasisteady solutions. For a quasisteady case the first two of Equations (12) are replaced by the single equation

$$V_n = V_{ni} \tag{18}$$

It is also necessary to use the definition of U as an auxiliary condition. This requires the average velocity in the Z direction within a drop to be zero. Using Equation (9) one can express the required condition in the form

$$\int \psi_i(R_0, Z)\,dZ = 0 \tag{19}$$

where R_0 refers to values of the cylindrical radial coordinate along the drop surface.

SOLUTIONS FOR THE STREAM FUNCTIONS

The stream function used in the region external to the liquid drops is an extension of functions developed previously (*7, 8*) for a similar problem, and is written in the form

$$\psi = \psi_0 + \psi_a \tag{20}$$

where

$$\psi_0 = \left(\frac{U}{2} - \frac{V}{2}\right) R^2 + \frac{V}{4} R^4 \tag{21}$$

with

$$V = \frac{2Q}{\pi} \tag{22}$$

ψ_0 represents the flow that would take place in the absence of the liquid drops. It satisfies the boundary conditions (11). The additional stream function ψ_a must then satisfy homogeneous boundary conditions on $R = 1$.

$$\psi_a = 0, \quad V_z = 0 \quad \text{on} \quad R = 1 \tag{23}$$

The function ψ_a is constructed by starting with the general solution of $E^4\psi = 0$ in spherical coordinates. These solutions are (*6*)

$$\psi = \sum_{n=2}^{\infty} C_n^{-1/2} (A_n r^n + B_n r^{-n+1} + C_n r^{n+2} + D_n r^{-n+3}) \tag{24}$$

The two singular terms of Equation (24) with factors r^{-n+1} and r^{-n+3}, $n = 2$, with the addition of certain nonsingular terms, are used to derive a pair of functions which satisfy Equations (23) and have singularities at the centers of each liquid drop. These functions are (*7*)

$$\psi^{(1)} = \sum_{n=-\infty}^{\infty} \frac{R^2}{2[R^2 + (Z - n\beta)^2]^{3/2}} + \left\{A_0R^4 + B_0R^2 + \sum_{m=1}^{\infty} [A_m R I_1(mkR) + B_m R^2 I_0(mkR)] \cos(mkZ)\right\}$$

$$\psi^{(2)} = \frac{1}{2}\frac{R^2}{[R^2 + Z^2]^{1/2}} + \frac{1}{2}\sum_{n=1}^{\infty}\left\{\frac{R^2}{[R^2 + (Z - n\beta)^2]^{1/2}} + \frac{R^2}{[R^2 + (Z + n\beta)^2]^{1/2}} - \frac{2R^2}{n\beta}\right\} + \left\{C_0R^4 + D_0R^2 + \sum_{m=1}^{\infty} [C_m R I_1(mkR) + D_m R^2 I_0(mkR)] \cos(mkZ)\right\} \tag{25}$$

where $k = 2\pi/\beta$. Substitution of Equations (25) in Equations (23) determines the A_m, B_m, C_m, D_m completely. (See reference 7 for explicit formulas.)

After satisfying the boundary condition, $\psi^{(1)}$ and $\psi^{(2)}$ are converted to spherical coordinates and two infinite series of functions are generated by taking derivatives with respect to Z. The singular parts of these series are equivalent to the sum over n of the terms with negative exponents in Equation (24). The derivative functions used are defined as

$$\psi_n^{(j)} = \frac{1}{(n-2)!} \frac{\partial^{n-2}\psi^{(j)}}{\partial z^{n-2}}; \quad n = 2, 3, 4, \ldots; \quad j = 1, 2 \tag{26}$$

Each of the $\psi_n^{(j)}$ are periodic in Z and satisfy Equation (23) and $E^4\psi = 0$.

The stream function ψ_a is expressed as a sum over the $\psi_n^{(j)}$ each multiplied by a coefficient which represents the unknown strength of the singularity in that $\psi_n^{(j)}$. The entire exterior stream function is then written in the form

$$\psi = \sum_{n=2}^{\infty} (E_n\psi_n^{(1)} + F_n\psi_n^{(2)}) + \psi_0 \tag{27}$$

The flow pattern inside every drop is the same. For the drop centered at the origin, the general solution [Equation (24)] is reduced to

$$\psi_i = \sum_{n=2}^{\infty} C_n^{-1/2}(\eta)\ (\overline{A}_n r^n + \overline{C}_n r^{n+2}) \tag{28}$$

to avoid infinite velocities at the origin. $\overline{A}_n$ and $\overline{C}_n$ are constants to be determined by the boundary conditions on the surface of the drop. When the boundary conditions on the surface of the drop centered at the origin are satisfied, the boundary conditions on the surface of every other spherical drop will also be satisfied because the exterior stream function is periodic in Z.

DRAG AND PRESSURE DROP

The drag on an axisymmetric body is given by (*9*)

$$D = \pi \int R^3 \frac{\partial}{\partial n}\left(\frac{E^2\psi}{R^2}\right) ds \tag{29}$$

where the integration is extended over the generating curve. When the stream function is written as in Equation (27), Equation (29) reduces to (*11*)

$$D = 4\pi F_2 \tag{30}$$

The pressure drop per particle is defined by

$$\Delta p = [p]_{\substack{R=R_0\\ Z=\beta/2}} - [p]_{\substack{R=R_0\\ Z=-\beta/2}} \tag{31}$$

The pressure may be determined to within a constant once ψ is known from the equations

$$\frac{\partial p}{\partial r} = \frac{1}{r^2}\frac{\partial}{\partial n}(E^2\psi)$$
$$\frac{\partial p}{\partial n} = (1-\eta^2)^{-1/2}\frac{\partial}{\partial r}(E^2\psi) \tag{32}$$

Integration of Equations (32) and substitution in Equation (31) result in

$$\Delta p = -8F_2 - 16E_2 - 4V\beta \tag{33}$$

A mean pressure gradient p_Z is defined by

$$p_Z = \frac{\Delta p}{\beta} = \frac{1}{\beta}(-8F_2 - 16F_2) - 4V \tag{34}$$

The last term in Equation (34) is the pressure drop for a Pouiselle flow of a uniform fluid with discharge $Q = \pi V/2$.

METHOD OF SOLUTION

An iterative technique is used which is similar to that developed for other free stream line problems (*12*). In the present case, an initial shape of the drops is first chosen, and a solution for the corresponding velocity field is found. This solution will in general yield nonzero velocities normal to the drop surfaces. These velocities are used to compute a new shape, for which a new solution for the velocity field is computed. This procedure is continued until a shape having vanishingly small normal velocities is obtained. The results are not linear in either the drop velocity U or the mean velocity $V/2$, and in addition the shape depends nonlinearly on the surface tension. Therefore superposition of solutions is not possible, and each case must be dealt with separately. The case of neutrally buoyant drops is of particular interest here because of its relationship to blood flow. Computations have been carried out for this case only.

For neutrally buoyant drops the drag is zero. Then from Equation (30)

$$F_2 = 0 \tag{35}$$

In order to achieve zero drag, the velocity of the centroid of each drop U and the average speed $V/2$ must have a certain ratio. This ratio is determined in the course of the solution and it replaces F_2 as an unknown. In the analysis and computations below, it is convenient to regard V as given and U as an unknown.

At each step of the solution, the problem is one of finding the velocity field for a given instantaneous shape of the drops. For this purpose a boundary method with least-square error (*13*) is used in which the boundary conditions are considered at a finite set of boundary points. The series ψ and ψ_i are truncated so that the number of equations is greater than the number of unknown coefficients. The boundary conditions at each point are satisfied approximately. The approximation is such that the errors in the entire set of equations are minimized in the least-squares sense.

In the resulting system of equations the unknowns are expressed as

$$X_n = VX_n^* \tag{36}$$

Defining

$$\delta^* = \frac{\delta}{V} = \frac{\delta'}{\rho\nu V'} \tag{37}$$

the dimensionless unknowns X_n^* become functions of β, λ, σ, and δ^*. The parameter δ^* is a measure of the surface tension in comparison to the viscous stresses.

In performing these numerical calculations the drop surface is specified by giving r_0, the radius of the drop, at equally spaced points in θ. The first and second derivatives of r_0 with respect to θ are then computed by using five-point approximations. These derivatives are used in computing α and H.

When the coefficients E_n, F_n, $\overline{A}_n$, $\overline{C}_n$ have been determined, the change in the drop shape in a time Δt is computed as

Table 1. Numerical Results

β	λ	σ	δ^*†	(r_0) max	$2U^*$	P^*	G^*
1.5	0.5	1	∞	0.500	1.78	0.074	0.012
		1	5	0.512	1.78	0.071	0.012
		1	2	0.534	1.78	0.069	0.011
		1	1	0.584	1.79	0.060	0.010
		10	∞	0.500	1.69	0.22	0.036
		10	1	0.581	1.70	0.20	0.033
	0.7	1	∞	0.700	1.55	0.42	0.070
		1	5	0.732	1.56	0.38	0.063
		1	2	0.793	1.58	0.32	0.053
		1	1	0.839	1.58	0.29	0.048
		10	∞	0.700	1.43	1.20	0.200
		10	5	0.728	1.43	1.17	0.195
4.0	0.5	1	∞	0.500	1.79	0.081	0.0050
		1	5	0.517	1.79	0.079	0.0049
		1	2	0.539	1.79	0.077	0.0048
		1	1	0.593	1.80	0.069	0.0043
	0.7	1	∞	0.700	1.56	0.56	0.035
		1	5	0.753	1.57	0.52	0.032
		1	2	0.892	1.62	0.38	0.024

† $\delta^* = \infty$ indicates results for spherical drops (*11*).

$$r_0(\theta, t + \Delta t) = r_0(\theta, t) + \left(V_{ri} - V_{\theta i} \frac{1}{r_0} \frac{dr_0}{d\theta} \right) \Delta t \tag{38}$$

The volume within the drop must be constant since the internal fluid is incompressible. In the numerical computations $r_0(\theta)$ was adjusted at the end of each cycle of computation to ensure constant volume.

After a steady state has been achieved, the drop shape and certain dimensionless variables are recorded, namely, U^*, P^*, and G^*. Dimensional quantities of interest are related to dimensionless coefficients as follows

$2U^*$ is the ratio of the drop velocity to the mean velocity of flow

$$2U^* = \frac{2U'}{V'} \tag{39}$$

The pressure drop $\Delta p'$ over a tube length βa is

$$\Delta p' = \frac{\rho \nu V'}{a} (P^* + 4\beta) \tag{40}$$

The mean pressure gradient p_z' is

$$p_z' = \frac{4\rho \nu V'}{a^2} (G^* + 1) \tag{41}$$

where

$$G^* = P^*/4\beta \tag{42}$$

RESULTS

Numerical results are summarized in Table 1 which gives the velocity ratio $2U^*$, the pressure drop coefficient P^*, the pressure gradient coefficient G^*, and the maximum radius of the drop as measured from the centroid. This maximum always occurs on the tube center line. Results for the case in which the drops are assumed to remain spherical (*8*) are included in Table 1 as $\delta^* = \infty$. It is significant that deformable drops ($\delta^* < \infty$) result in a lower pressure gradient coefficient than that obtained for spherical drops ($\delta^* = \infty$) of the same viscosity and volume. For a case such as that shown in Figure 4 this decrease is about 20 to 30% of the additional pressure gradient. As the velocity of the flow increases, the additional pressure drop decreases. This constitutes a mechanism of non-Newtonian behavior in the sense that the resistance (pressure drop divided by discharge) decreases as the discharge increases. Recent studies (*14, 15*) of the passage of a close-fitting elastic particle through a fluid-filled cylindrical tube show similar results. Direct measurements of the resistance of whole blood or suspensions of red cells in capillary size glass tubes have also been reported (*16, 17*). These studies, conducted at flow rates considerably in excess of those expected in vivo, do not show any variation of resistance with flow rate. A possible explanation for this can be found in recent measurements of the deformation of red blood cells flowing through glass tubes (*18*). The experiments showed that the deformation of the cells increases with increasing flow rate. This is in agreement with the present numerical results, but in the experimental study the cell shape did not continue to change at flow rates above 1 mm./sec. At high flow rates the shape of the cells remains fixed and the discharge remains proportional to the pressure gradient.

Typical examples of the shapes computed are shown in Figures 2, 3, and 4 along with the shapes computed by a perturbation procedure (*11*). It is noteworthy that the shapes computed (for example, Figure 4) are very similar to the shapes of red blood cells observed in vivo (*19*) and in vitro (*20*). When the red cell is observed to have a shape similar to Figure 4, it appears that it is moving with the plane of the disk parallel to the tube axis (*19*). The shape observed may then be a distorted disk rather than the axisymmetric shapes computed for the drops in the present analysis.

CONCLUSIONS

The results obtained here are of interest both for their quantitative aspects and for the demonstration of non-Newtonian behavior which is attributable to the deformability of the suspended elements. The importance of deformability of red cells on the apparent viscosity of blood has been recently discussed from a more physiological viewpoint (*21* to *23*). Since an appreciable part of the total resistance of blood flow occurs in the capillaries, deformability of the red cells is important with regard to the ability of cells to pass through a capillary bed. It is known, for example, that sickle cell anemia, which is characterized by increased rigidity of the red cell, can cause the flow through the capillary bed to be severely restricted. The red cell is

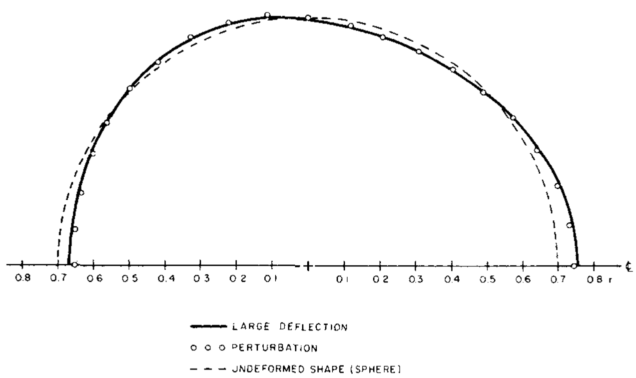

Fig. 2. Computed drop shapes $\beta = 2.0$, $\lambda = 0.7$, $\sigma = 1$, $\delta^* = 5$.

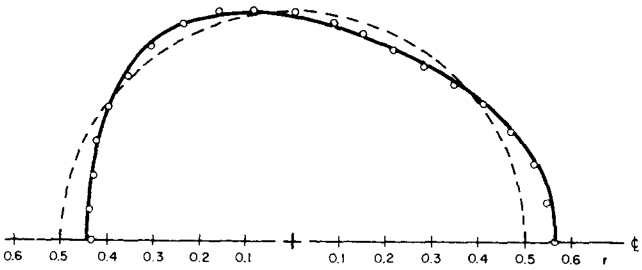

Fig. 3. Computed drop shapes $\beta = 1.5$, $\lambda = 0.5$, $\sigma = 0$, $\delta^* = 1$.

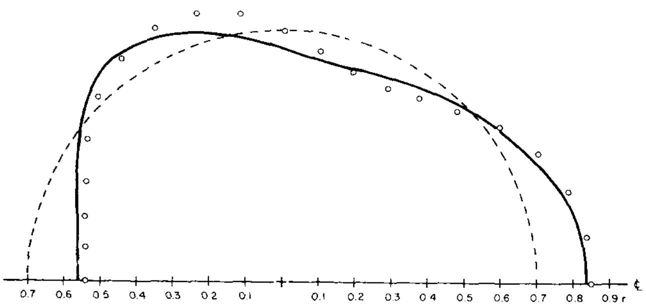

Fig. 4. Computed drop shapes $\beta = 1.5$, $\lambda = 0.7$, $\sigma = 0$, $\delta^* = 1$.

normally quite deformable and the membrane tension of a red cell is small (*24*); however the elastic forces tending to maintain the shape of the cell may be regarded as playing the same role as the surface tension in the present model.

ACKNOWLEDGMENT

This paper is based on the doctoral dissertation by W. A. Hyman at Columbia University, 1970. The research was supported by the Office of Naval Research under Contract No. N00014-67-A-0108-0003.

NOTATION

$A_n, B_n, C_n, D_n, E_n, F_n$ = constants
a = radius of tube
$C_n^{-1/2}$ = Gegenbaur polynomial
D = drag
E^4 = differential operator [see Equation (6)]
G^* = pressure gradient coefficient
H = mean curvature
I_0, I_1 = modified Bessel function of first kind
P^* = pressure drop coefficient
p = pressure
Δp = pressure drop per particle
p_Z = mean pressure gradient
Q = discharge
R, Z = cylindrical coordinates
$R_0(Z)$ = drop surface in cylindrical coordinates
R_1, R_2 = principal radii of curvature
r, θ = spherical coordinates
$r_0(\theta)$ = drop surface in spherical coordinates
t = time
U = velocity of fluid drops
U^* = U/V
V = twice the mean velocity of flow
$\mathbf{V}'$ = velocity
∇ = gradient operator

Greek Letters

α = angle between normal and radial directions
β = ratio of drop spacing to tube radius
δ^*, δ = dimensionless surface tensions
λ = ratio of drop size to tube radius
μ = absolute viscosity
ν = kinematic viscosity
ρ = density
σ = viscosity ratio
τ = stress
ψ = stream function

Subscripts

R, Z = components in cylindrical coordinates
r, θ = components in spherical coordinates
n, t = components normal and tangential to drop surface
i = denotes inside a drop

Superscript

$'$ = dimensional quantity

LITERATURE CITED

1. Skalak, R., *J. Fluid Mech.*, **42**, 527 (1970).
2. Bretherton, F. P., *ibid.*, **10**, 166 (1961).
3. Davies, R. M., and G. I. Taylor, *Proc. Roy. Soc. London*, **A200**, 375 (1949).
4. Cox, B. G, *J. Fluid Mech.*, **14**, 81 (1962).
5. Goldsmith, H. L., and S. G. Mason, *ibid.*, **14**, 42 (1962).
6. Haberman, W. L., and R. M. Sayre, *David Taylor Model Basin Rept. No. 1143* (1958).
7. Wang, H., and R. Skalak, *J. Fluid Mech.*, **38**, 75 (1969).
8. Hyman, W. A., and R. Skalak, *Tech. Rept. No. 3*, Proj. No. NR 062-393, Dept. Civil Eng. Eng. Mech., Columbia Univ. (1969).
9. Happel, J., and H. Brenner, "Low Reynolds Number Hydrodynamics," Prentice-Hall, Englewood Cliffs, N.J. (1965).
10. Timoshenko, S., and S. Woinowsky-Krieger, "Theory of Plates and Shells," McGraw-Hill, New York (1959).
11. Hyman, W. A., and R. Skalak, *Tech. Rept. No. 5*, Proj. No. NR062-393, Dept. Civil Eng. and Eng. Mech., Columbia Univ. (1970).
12. Robertson, J. M., "Hydrodynamics in Theory and Application," p. 421, Prentice-Hall, Englewood Cliffs, N. J. (1965).
13. Collatz, L., 'The Numerical Treatment of Differential Equations," 3rd edit., Springer-Verlag (1960).
14. Lighthill, M. J., *J. Fluid Mech.*, **34**, 113 (1968).
15. Fitz-Gerald, J. M., *Proc. Roy. Soc. London*, **B174**, 193 (1969).
16. Prothero, J., and A. C. Burton, *Biophys. J.*, **1**, 565 (1961).
17. Braasch, D., and W. Jennett, in "5th European Conference on Microcirculation," H. Harders, Ed., 109 (1969).
18. Hockmuth, R. M., R. N. Marple, and S. P. Sutera, *Microvascular Res.*, **2**, 409 (1970).
19. Skalak, R., and P.-I. Branemark, *Science*, **164**, 717 (1969).
20. Marple, R. N., and R. M. Hochmuth, paper presented at Eighth Intern. Congr. Med. Biol. Eng., Chicago (July 1969).
21. Chien, S., S. Usami, R. J. Dellenbach, and M. I. Gergersen, *Science*, **157**, 827 (1967).
22. Schmid-Schonbein, H., R. Wells, and J. Goldstone, *Circulation Res.*, **25**, 131 (1969).
23. Fitz-Gerald, J. M., *J. Appl. Physiol.*, **27**, 912 (1969).
24. Fung, Y. C., *Federation Proc.*, **25**, 1761 (1966).

Manuscript received November 2, 1970; revision received April 2, 1971; paper accepted April 5, 1971. Paper presented at AIChE Chicago meeting.